RIN transfer in 2nd-order distributed amplification with ultralong fiber lasers

Mercedes Alcón-Camas[1] and Juan Diego Ania-Castañón[2,*]

[1]*Photonics Research Group, School of Engineering and Applied Science, Aston University, Aston Triangle, Birmingham, B4 7ET, UK*
[2]*Instituto de Óptica "Daza de Valdés," CSIC, C/ Serrano 121, 28006 Madrid, Spain*
**juan.diego@io.cfmac.csic.es*

Abstract: We investigate numerically the effect of ultralong Raman laser fiber amplifier design parameters, such as span length, pumping distribution and grating reflectivity, on the RIN transfer from the pump to the transmitted signal. Comparison is provided to the performance of traditional second-order Raman amplified schemes, showing a relative performance penalty for ultralong laser systems that gets smaller as span length increases. We show that careful choice of system parameters can be used to partially offset such penalty.

OCIS codes: (190.4370) Nonlinear optics, fibers; (060.3510) Lasers, fiber; (250.4480) Optical amplifiers.

References and links

1. M. N. Islam, "Raman amplifiers for telecommunications," IEEE J. Sel. Top. Quantum Electron. **8**(3), 548–559 (2002).
2. J. Bromage, "Raman amplification for fiber communications systems," J. Lightwave Technol. **22**(1), 79–93 (2004).
3. J. D. Ania-Castañón, T. J. Ellingham, R. Ibbotson, X. Chen, L. Zhang, and S. K. Turitsyn, "Ultralong Raman fiber lasers as virtually lossless optical media," Phys. Rev. Lett. **96**(2), 023902 (2006).
4. J. D. Ania-Castañón, "Quasi-lossless transmission using second-order Raman amplification and fibre Bragg gratings," Opt. Express **12**(19), 4372–4377 (2004), http://www.opticsinfobase.org/abstract.cfm?URI=oe-12-19-4372.
5. A. E. El-Taher, J. D. Ania-Castañón, V. Karalekas, and P. Harper, "High efficiency supercontinuum generation using ultra-long Raman fiber cavities," Opt. Express **17**(20), 17909–17915 (2009).
6. M. Alcón-Camas, A. E. El-Taher, H. Wang, P. Harper, V. Karalekas, J. A. Harrison, and J. D. Ania-Castañón, "Long-distance soliton transmission through ultralong fiber lasers," Opt. Lett. **34**(20), 3104–3106 (2009).
7. J. Scheuer, and A. Yariv, "Giant fiber lasers: a new paradigm for secure key distribution," Phys. Rev. Lett. **97**(14), 140502 (2006).
8. C. R. S. Fludger, V. Handerek, and R. J. Mears, "Pump to Signal RIN Transfer in Raman Fiber Amplifiers," J. Lightwave Technol. **19**(8), 1140–1148 (2001).
9. B. Bristiel, S. Jiang, P. Gallion, and E. Pincemin, "New model of noise Figure and RIN transfer in fiber Raman amplifiers," IEEE Photon. Technol. Lett. **18**(8), 980–982 (2006).
10. M. D. Mermelstein, K. Brar, and C. Headley, "RIN Transfer Measurement and Modeling in Dual-Order Raman Fiber Amplifiers," J. Lightwave Technol. **21**(6), 1518–1523 (2003).
11. M. Krause, S. Cierullies, H. Renner, and E. Brinkmeyer, "Pump-to-Stokes RIN transfer in Raman fiber lasers and its impact on the performance of co-pumped Raman amplifiers," Opt. Commun. **260**(2), 656–661 (2006).
12. V. Kalavally, I. D. Rukhlenko, M. Premaratne, and T. Win, "Analytical study of RIN transfer in pulse-pumped Raman amplifiers," J. Lightwave Technol. **27**(20), 4536–4543 (2009).
13. S. K. Turitsyn, S. A. Babin, A. E. El-Taher, P. Harper, D. V. Churkin, S. I. Kablukov, J. D. Ania-Castañón, V. Karalekas, and E. V. Podivilov, "Random distributed feedback fibre laser," Nat. Photonics **4**(4), 231–235 (2010).

1. Introduction

Conventional silica optical fibers are susceptible to Raman scattering, with a Stokes frequency at ~13.2 THz from that of the pump, which can be used to provide amplification over a chosen range of wavelengths. The most important advantages of distributed optical fiber Raman amplifiers [1,2] over traditional lumped optical amplification are their improved noise performance and extended bandwidth. The fact that conventional optical fiber can be

#133696 - $15.00 USD Received 19 Aug 2010; revised 9 Oct 2010; accepted 10 Oct 2010; published 26 Oct 2010

efficiently Raman pumped brings the opportunity of upgrading existing transmission systems through the implementation of Raman amplification, whether on its own or combined with other existing amplification solutions, increasing system performance and capacity. Recently, ultralong Raman fiber lasers (URFLs) [3–7], in which transmission fiber acts as an ultralong laser cavity that is used for signal amplification, have been shown to be able to provide reduced signal power excursion with single-wavelength pumping, improving noise performance and presenting itself as an interesting alternative to other high-order Raman amplification schemes. Among the challenges of distributed Raman amplification, an important one is pump-to-signal relative intensity noise (RIN) [8–12] transfer, caused by fluctuations on the pump power that lead to a time-dependent variation of signal gain and are thus imprinted in the signal.

In this paper, through the development of a new numerical model for higher order distributed Raman amplifiers applicable to ultralong Raman fiber lasers, we investigate the effect of system design parameters, such as span length, pump distribution and fiber Bragg gratings (FBGs) reflectivity, on the relative intensity noise transfer performance of the system.

2. Theoretical model

The presented 2nd-order model for RIN transfer is a generalization of previously developed descriptions [8–10], with the inclusion of some typically neglected effects that can have an important impact in RIN transfer in the case of ultralong lasers, such as Rayleigh backscattering. In this manuscript we focus on the study of two particular Raman-amplified systems based on standard single-mode fiber (SMF), schematically described in Fig. 1.

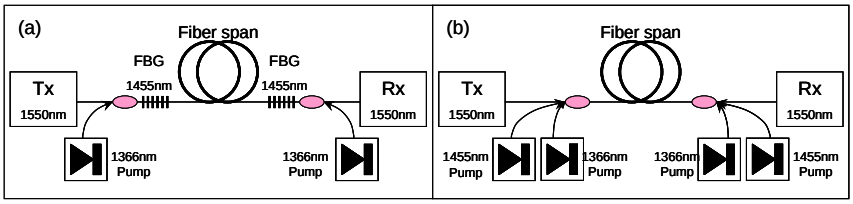

Fig. 1. Schematic description of the studied pumped Raman amplifier systems. (a) Ultralong Raman fiber laser. (b) Equivalent power distribution system with dual pumping scheme.

The first system corresponds to an SMF-based bi-directionally pumped URFL. It involves a conventional standard optical fiber confined between a pair of fiber Bragg grating (FBG) reflectors with a central wavelength of 1455 nm, corresponding to the first Raman Stokes of the pump source. Reflectivity will be considered a variable in our study, as well as the length of the fiber span, which ranges from 1 to 100 km. The pump power at 1366 nm is coupled into the system through WDMs. The wavelength of the transmitted signal is at 1550 nm, corresponds to the second Stokes of the pump source. As the pump power injected at 1366 nm overcomes the threshold for the fiber cavity, a first Stokes component around 1455 nm is generated and trapped between the grating reflectors. This component will behave as a second pump source, providing a wide Raman gain bandwidth to the transmitted signal, located around the second Stokes wavelength of 1550 nm. This structure provides quasi-lossless transmission around 1550 nm for an optimally adjusted pump power [3,4,6].

The second system involves an identical fiber span to the previous one, but with no reflectors at all, hence no laser cavity. The optical fiber is bi-directionally pumped with pumps at 1366 nm and 1455 nm. The transmitted signal is again at 1550 nm, corresponding to the second Stokes of the 1366 nm pumps and the first Stokes of the 1455 nm pumps.

In order to ensure a fair comparison between the performance of both systems, we operate the second one as follows. We increase the pump power at 1366nm to the same level as we would have done for the first system for an identical span length and signal power. Then, we calculate the initial power at 1455 nm at each end of the fiber span for our first system and use

#133696 - $15.00 USD Received 19 Aug 2010; revised 9 Oct 2010; accepted 10 Oct 2010; published 26 Oct 2010

exactly the same 1455 nm power value for the pumps of our second system. This allows us to generate an equivalent amplifier system to the first one with exactly the same power distribution for 1366 nm, 1455 nm and the signal 1550 nm, but using an extra bi-directional pump source at 1455 nm instead of using FBGs. Hence, average power distributions inside the two amplifiers are identical, which will make it possible to perform a direct comparison of their respective RIN transfer performances. Therefore any difference on the RIN transfer values between these two systems is expected to come from the impact of generating the secondary pump in the ultralong laser cavity instead of using a dual wavelength pumping scheme. Following the usual approach in published literature [8–12], the RIN is defined as the ratio of the time-averaged mean square value of the power fluctuations to the squared average power of the particular spectral component. We are interested in the spectral distribution of pump-to-signal RIN transfer, monitored through the RIN transfer function defined as:

$$H_{2nd}(\omega) = \left| \frac{RIN_{Signal}^{Out}(\omega)}{RIN_{Pump}^{In}(\omega)} \right| \tag{1}$$

where the corresponding RIN spectra are calculated from the ratio of the squared spectral density of the amplitude noise to the squared average power of each component. The ordinary differential equations that describe mathematically our model are subdivided in two groups. On the one side we have a set of ODEs describing the average power evolution of pumps, signal and propagation noise along the length of the fiber for a second order Raman amplifier (with their respective boundary conditions set in accordance to the rules mentioned above to make the comparison fair). This set of equations takes into account all relevant effects, including pump depletion, amplified spontaneous emission (ASE) and double Rayleigh scattering (DRS) noise. A detailed description of the model and its solution can be found in reference [4]. On the other hand, the evolution of the spectral density of amplitude noise in a second-order amplification scheme can be described through a second set of ODEs:

$$\frac{dn_1^{\pm}}{dz} + id_1^{\pm}\omega n_1^{\pm} = \mp\alpha_1 n_1^{\pm} \mp g_1 \frac{\nu_1}{\nu_2} P_1^{\pm}(n_2^{+} + n_2^{-}) \mp g_1 \frac{\nu_1}{\nu_2}(P_2^{+} + P_2^{-}) n_1^{\pm} \pm \varepsilon_1 n_1^{\mp} \tag{2}$$

$$\frac{dn_2^{\pm}}{dz} + id_2^{\pm}\omega n_2^{\pm} = \mp\alpha_2 n_2^{\pm} \pm g_1 P_2^{\pm}(n_1^{+} + n_1^{-}) \pm g_1 n_2^{\pm}(P_1^{+} + P_1^{-}) \mp g_2 \frac{\nu_2}{\nu_S} P_2^{\pm} n_S \mp g_2 \frac{\nu_2}{\nu_S} n_2^{\pm} P_S \pm \varepsilon_2 n_2^{\mp} \tag{3}$$

$$\frac{dn_S}{dz} = -\alpha_S n_S + g_2 P_S (n_2^{+} + n_2^{-}) + g_2 n_S (P_2^{+} + P_2^{-}) + \varepsilon_S n_S^{-} \tag{4}$$

where the n_i represent the spectral density of amplitude noise, the group velocity for each spectral component is represented by υ_i, the term $d_i^{\pm} = 1/\upsilon_S \pm 1/\upsilon_i$ accounts for the effect of the relative propagation speeds of the different spectral components, z is the length measured along the fiber span, P_i represent the pump and signal powers at the different frequencies (obtained through the solution of the set of ODEs in [4]), with the subscript "1", referring to the primary pump at 1366 nm, "2" being the first Stokes at 1455 nm, and "s" referring to the signal at 1550 nm, whereas n_i represent the spectral densities of the amplitude noise. The attenuation coefficient, α_i, is in units of km^{-1}. The optical frequency for each spectral component is represented by ν_i. The strength of the coupling between the pumps and the signal are determined by g_i, the Raman gain coefficients for the fiber, which have units of W^{-1}

#133696 - $15.00 USD Received 19 Aug 2010; revised 9 Oct 2010; accepted 10 Oct 2010; published 26 Oct 2010

Km^{-1}. The pump modulation frequency is represented by ω. The signs ± correspond to components propagating in forward (+) or backward (-) direction. Here and through this paper is assumed that the signal propagates in the forward + z direction. ε_i are the Rayleigh backscattering coefficients of the fiber at each particular frequency. The cavity design parameters are introduced in the boundary conditions. The FBGs are located at z = 0 and z = L and have reflectivities R_1 and R_2 respectively. Each of the two schemes is described by a different set of boundary conditions:

$$\text{For scheme 1: } n_1^+(0) = n_{10}; n_1^-(0) = n_{20}; n_2^+(0) = R_1 n_2^-(0); n_2^-(L) = R_2 n_2^+(L); n_S(0) = 0 \quad (5)$$

$$\text{For scheme 2: } n_1^+(0) = n_{10}^+; n_1^-(0) = n_{10}^-; n_2^+(0) = n_{20}^+; n_2^-(L) = n_{20}^-; n_S(0) = 0 \quad (6)$$

The complete system of equations can be expanded into its real and imaginary parts and solved through a number of methods. In our case we have used a finite element method with spline collocation at Gaussian points. Simulation parameters are summarized on Table 1.

Table 1. Simulation parameters

Wavelength (nm)	g (W^{-1} km^{-1})	α (dB/km)	ε (km^{-1})	d^+ (s/m)	d^- (s/m)
1366	0.51	0.33	$1.0\text{x}10^{-4}$	$2.8\text{x}10^{-9}$	$1.0\text{x}10^{-5}$
1455	0.36	0.26	$6.0\text{x}10^{-5}$	$1.35\text{x}10^{-9}$	$1.0\text{x}10^{-5}$
1550	-	0.20	$4.3\text{x}10^{-5}$	-	-

3. Results and discussion

Unless otherwise stated, all the calculations for the numerical simulation work shown on this manuscript are subject to the zero-loss condition; that is, total pump powers are automatically adjusted to obtain identical output signal power to the input one, regardless of span length, pump power distribution or any other parameter of the amplifier system.

The numerical results for the RIN transfer value for different span lengths are graphically represented below. Figure 2(a) the ultralong laser cavity with 90% reflectivity FBGs and Fig. 2(b) the dual pumping scheme with no FBGs. The value of transmitted signal is 1 mW in both cases, ensuring low pump depletion. The final obtained transfer function is independent of the initial RIN of the laser pumps, as long as this is set to be identical for the different sources. The only variable parameter is the length of the fiber span; otherwise the forward-backward pump ratio distribution is symmetric and the zero-loss condition is applied.

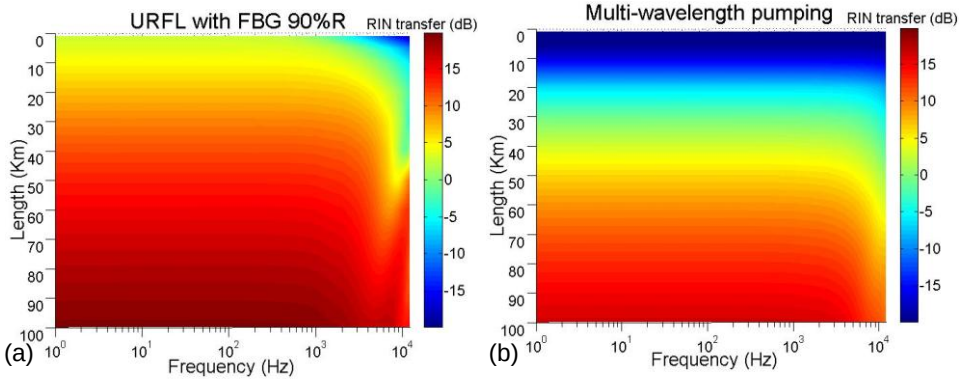

Fig. 2. RIN transfer value at several span lengths for (a) laser cavity with 90% FBGs and (b) fiber span dual pumping scheme without reflectors.

As a general trend, the maximum RIN transfer value increases with length regardless of whether the Raman amplifier is a laser cavity, Fig. 2(a), or a simple fiber span without

#133696 - $15.00 USD Received 19 Aug 2010; revised 9 Oct 2010; accepted 10 Oct 2010; published 26 Oct 2010

reflectors, Fig. 2(b). The maximum RIN value at 75 km, for the cases of laser cavity with FBGs at 90% reflectivity and fiber span without reflectors, are 17 dB and 12.25 dB respectively (i.e. RIN transfer is 4.75 dB higher in the ultralong cavity). A penalty in terms of maximum value of the RIN transfer for the ultralong laser cavity in comparison with the dual pumping scheme without reflectors is observed in all cases. The differences between the performances of both schemes, though, are reduced with increasing span length. A major distinction between both systems is the decline of the RIN transfer value at higher modulation frequencies. Whilst in the case of the dual pumping scheme without reflectors the RIN transfer drops gradually with increasing modulation frequency, in the case of the laser cavity the RIN transfer value shows a fluctuating behavior towards lower values, especially for the longer span lengths. A direct comparison of the RIN transfer value between both systems is graphically presented in Fig. 3(a) for two particular cases, the RIN transfer value at its maximum (lowest modulation frequency) and at 4 kHz. The RIN transfer value in both systems converges for longer span lengths. Also the value of the RIN transfer at 4 kHz is lower in the case of dual pumping scheme than the ultralong cavity. Furthermore, as Fig. 3(b) shows, the cutoff frequency (taken here as the frequency at which the RIN transfer has dropped 2 dB below its maximum value for the particular configuration) is lower for the laser cavity case than for the fiber span without reflectors, given the same fiber length and power conditions. As in the case of a standard amplifier, the cut-off frequency is dependent on dispersion (through pump walk-off) fiber loss, and shows a strong dependence on span lengths mainly for short spans below 40 km in the case of standard fiber [8]. The faster oscillating behavior and lower cut-off frequency in the case of the ultralong cavity are illustrated on Fig. 3(c).

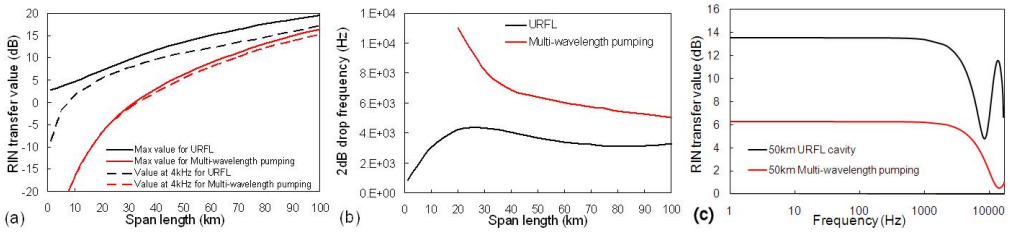

Fig. 3. (a) Maximum RIN transfer value and value at 4 kHz at versus span length for the two considered schemes, (b) 2 dB drop frequency versus span length for the two considered schemes, (c) subset of results from figure 2(a)

The unusual behaviour of the oscillations in the cavity compared to the case of a standard second-order amplification scheme can be attributed to a combination of the presence of peaks corresponding to the cavity round-trip and the fact that oscillations in the backward-propagating components are reinforced due to the boundary conditions set by the FBG reflectors, which feed them back into the cavity.

The pump power split has a clear impact on the RIN transfer value. For the case of a laser cavity, shown in Figs. 4(a) and 4(c) the optimum pump split for the lowest RIN transfer value is 80% forward - 20% backward, with a maximum RIN transfer function value of 16.83 dB. Using any pump power split other than 80% / 20% causes relatively small variations of up to 0.9 dBs to the RIN transfer value. Symmetric pumping is, on the other hand, the best option for the case of the dual-wavelength pumping scheme without reflectors, as shown in Fig. 4(b) and 4(c), with a RIN transfer value of 12.25 dB. In this case, though, the RIN transfer function is much more sensitive to deviations from the optimal case, and can go up to 2.6 dB higher if we move away from the symmetrical configuration. The RIN transfer value drops continuously for higher modulation frequencies in all the cases where the major pump contribution is from the backward pump (pump ratio close to 0), whereas forward pumping leads to oscillations in the RIN transfer at higher frequencies, especially in the case of a laser cavity, increasing as well the 2 dB drop frequency for the case of dual pumping without

#133696 - $15.00 USD Received 19 Aug 2010; revised 9 Oct 2010; accepted 10 Oct 2010; published 26 Oct 2010

reflectors. As before, such drop appears at lower frequencies in the case of a laser cavity than the dual pumping scheme without reflectors. As well, the oscillations of the RIN transfer function are stronger for the case of laser cavity.

The effect of the pump split is shown on Fig. 4 for the cases of (a) laser cavity with 90% reflectivity FBGs and (b) dual pumping scheme without reflector. The value of transmitted signal is the same as previously, 1 mW. The span length is fixed at 75 km. The pump ratio is defined as the ratio of the forward pump power to the total pump power.

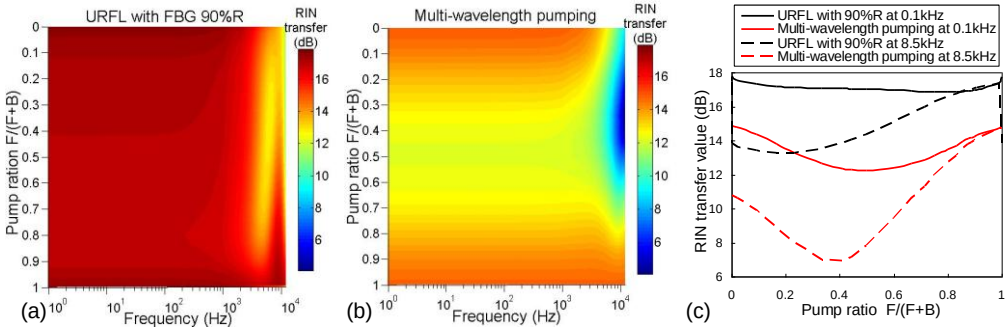

Fig. 4. RIN transfer value vs. pump ratio and Frequency for the case of (a) a 75km laser cavity with 90% reflectors, (b) a 75km dual-wavelength second-order pumping scheme without reflectors and (c) subset results from (a) and (b).

Grating reflectivity also plays an important role on the transfer of RIN. Fig. 5(a) shows the RIN transfer values in a 75 km ultralong laser cavity as grating reflectivity is varied from 0.1% to 100%. These results were, as before, calculated using a 1 mW forward transmitted signal. As observed in the previous results and Fig. 5(c), the 2 dB drop frequency is lower for higher reflectivies. A subset of the results shown on Fig. 5(a) is plotted on Fig. 5(b). From the figure we can observe that at low frequencies, the maximum value of the RIN transfer is set at 15% reflectivity. At higher modulation frequencies, such as 6 kHz, the worst case moves to lower FBGs reflectivity, 5%. The fact that cavities with relatively low reflectivity show worse RIN transfer performance than higher reflectivity may have interesting implications, for example, in areas such as that of random feedback ultralong Raman fiber lasers [13]. Maximum care should be provided in order to minimize any unwanted reflectivity in an experimental system.

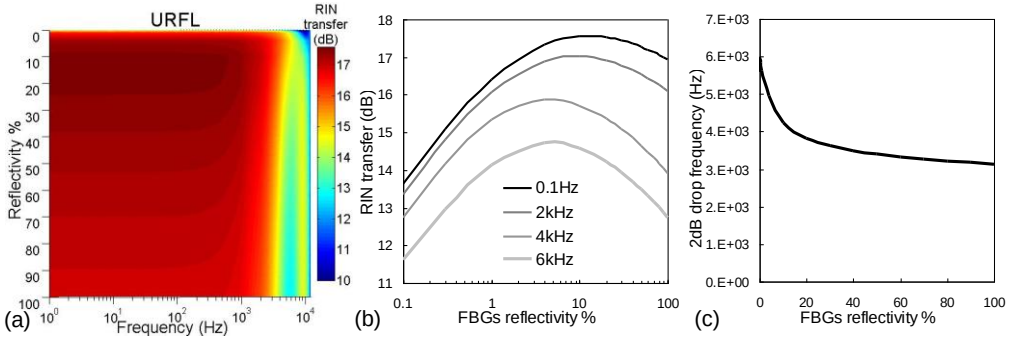

Fig. 5. (a) RIN transfer value vs. reflectivity and frequency for a 75 km laser cavity for different FBG reflectivities. (b) Subset of RIN transfer value vs. FBG reflectivity for different frequencies. (c) 2 dB drop frequency vs. FBGs reflectivity for the same cavity.

4. Conclusion

We have presented a numerical study of RIN transfer in second-order distributed Raman amplifiers, with special attention to ultralong Raman fiber lasers (URFL). The new numerical

#133696 - $15.00 USD Received 19 Aug 2010; revised 9 Oct 2010; accepted 10 Oct 2010; published 26 Oct 2010

model developed allows us to achieve a better understanding of how the design parameters of an ultralong laser cavity affect the RIN transfer performance of the system.

As expected, span length has a major impact on RIN transfer, increasing transfer for longer lengths regardless of the second-order configuration studied, but interestingly, the maximum RIN transfer value reached at low modulation frequencies asymptotically converges towards a common value for long lengths for the different configurations studied. URFLs display a performance penalty in comparison to standard multiwavelength-pumped second-order amplifiers, but also a rather different response to system parameter variation, being in general more robust to pump asymmetries as observed from Fig. 4. The maximum RIN transfer value in URFLs is not linked to the highest FBG reflectivity, but in fact, happens at relative low reflectivity of 15%. Pump split is also a key parameter which affects the maximum value of the RIN transfer function in different degrees depending on whether we are using a laser cavity or a dual-wavelength pumping scheme without reflectors. In addition, it is also related to the oscillating behavior of the RIN transfer function at higher frequencies, which becomes more obvious as the relative contribution of forward pumping increases.

Finally, we have observed that the cutoff frequency for the RIN transfer function, taken as the frequency at which the RIN transfer has dropped 2 dB below its maximum value for the particular configuration, is reduced not only with increasing span length, but also with increasing FBG reflectivity. In addition, cavities with relative low reflectivity show worse RIN transfer performance than higher reflectivity ones, which might have interesting implications in the future design and implementation of low-reflectivity systems making use of random distributed feedback.

Acknowledgements

The authors wish to thank the financial support of Ministerio de Ciencia e Innovación (MICINN) through grant TEC2008-05791 and of Engineering and Physical Sciences Research Council (EPSRC) through grant EP/E015646/1.

#133696 - $15.00 USD Received 19 Aug 2010; revised 9 Oct 2010; accepted 10 Oct 2010; published 26 Oct 2010